Defense Technical Information Center Compilation Part Notice

ADP011153

TITLE: Perspectives of Phase-Portraits in the Detection of Compressor Instabilities-Inception of Stall

DISTRIBUTION: Approved for public release, distribution unlimited

This paper is part of the following report:

TITLE: Active Control Technology for Enhanced Performance Operational Capabilities of Military Aircraft, Land Vehicles and Sea Vehicles [Technologies des systemes a commandes actives pour l'amelioration des performances operationnelles des aeronefs militaires, des vehicules terrestres et des vehicules maritimes]

To order the complete compilation report, use: ADA395700

The following component part numbers comprise the compilation report:
ADP011101 thru ADP011178

PERSPECTIVES of PHASE-PORTRAITS in the DETECTION of COMPRESSOR INSTABILITIES – INCEPTION of STALL.

M. D'ISCHIA*; F.A.E. BREUGELMANS
VON KARMAN INSTITUTE
72, Ch. de Waterloo
B-1640 Rhode St. Genese
Belgium
* Presently Universita di Napoli "Federico II".

ABSTRACT

The operative range of axial-flow compressors is limited by the onset of instabilities, namely rotating stall and surge that arise when the mass flow is reduced at constant rotational speed. The difficulties in correctly predicting the point of stall onset have made it necessary to establish a limit line on the performance map that cuts out operative points of high efficiencies. The particular behavior of this non-linear complex-but-structured phenomenon has suggested a scientific approach with the tools of Chaos theory. The result given by the Phase-Space reconstruction from experimental time series has suggested the possibility of applying this technique, not only to characterize the system's dynamics, but also for monitoring purposes. The experiments have been planned to capture the transition from clean flow to stalled conditions. The Phase-Portrait of the different types of stall is presented. The results from the different sensors are compared and an indicator for stall inception detection presented.

INTRODUCTION

Rotating stall has been widely investigated, both theoretically and experimentally. Recent experiments on the inception and development of stall cells are reported in [2,9,11,12,17,18,19,20,37]. Generally, stall inception can be experimentally detected as a small cell whose wave shape is obtained from a low pass filtering of a high frequency response sensor. It is, however, difficult to avoid stall upon recognition of the small cells because it takes only a few rotor revolutions for the full cell to develop: the hysteresis in the pressure rise characteristics makes it longer to recover under any active action. Garnier et al.[11,12] have investigated this phenomenon on two low speed and one high speed compressor with spatially and temporally resolved measurements. They found that rotating stall was preceded by a period in which small amplitude waves were observed travelling around the circumference at a speed slightly less that the fully developed cell's speed. The evolution into full cell was smooth and without sharp variations. The waves were clearer, for the multistage compressor, in the stage that stalled first. According to their results these waves were detectable 10 to 200 rotor revolutions before the onset and can be used for active control purposes. The data fitted the model by Moore and Greitzer [27] both qualitatively and quantitatively. This technique requires as many probes as the number of spatial harmonics to be examined. In the cited work 8 hot wire were necessary.
Rotating stall is a phenomenon that has also widely investigated theoretically during the last 40 years [10,16,25,26,27]. Recent numerical studies, McCaughan [25], on the Moore and Greitzer [27] model, have shown the importance of both spatial and temporal non-linearities already at the early stage of rotating stall inception. McCaughan [26] presents a parametric study of a simplified version of the same model. For a given set of parameters the final state, reached by a compressor when it goes unstable, strongly depends on the initial conditions. In the same study, strange attractors are thought to be possible for rotating stall. All these aspects suggest the possibility of an underlying chaotic dynamics in rotating stall in axial-flow compressors. From this point of view a compressor may be regarded as a non-linear, open, externally driven, dissipative dynamical system that experiences transitions to different dynamics as an external parameter, in this case the mass flow, is varied.
The applicability of the Phase-Portrait representation and the properties has been studied in [3,4,17,29,30,31,32]. A few concepts have to be mentioned shortly such as: Deterministic Chaos, Dimensions, Attractor, and Phase-Portrait reconstruction, which are used in the paper.

DETERMINISTIC CHAOS.

Chaos stands for states of irregularity and disorder. The appellation deterministic for a dynamic system implies the existence of a prescription, either in terms of difference or differential equation, that allows to predict the future behavior of the system starting from a given initial condition. The two terms seem to be in contradiction as one would normally think that only regular motions belong to the class of deterministic systems The idea is that the different structures possible for rotating stall for different values of the mass flow,

Paper presented at the RTO AVT Symposium on "Active Control Technology for Enhanced Performance Operational Capabilities of Military Aircraft, Land Vehicles and Sea Vehicles", held in Braunschweig, Germany, 8-11 May 2000, and published in RTO MP-051.

are chaotic states for the physical system. Examples of classic observations of rotating stall can be found in [2,11,22,23,24].

DISSIPATIVE DYNAMIC SYSTEMS

Consider a dynamic system for which each value of the variable represents one of the degrees of freedom of the system. The state of the system can be seen as represented, at a given instant in time, by a point or a vector in the Phase-Space that is the space in which all possible states for the system are represented. The property of dissipative systems dictates that they will settle from some transient to a simpler steady state response. Their trajectories in the Phase-Space reduce in volume, so that the flow contracts onto a set of lower dimension called attractor. A qualitative description of the system's dynamic is obtained through a geometrical description of the trajectories on the attractor. As an example, one could refer to the condition of a damped pendulum after a transient: the trajectory evolves in time starting from a given initial condition and is attracted to a fixed point coinciding with rest condition for the pendulum (**Fig.1**). The trajectory can be presented in a velocity – position graph. Systems undergoing periodic states will show a limit cycle or n-dimensional tori as attractors. Strange attractors are typical of chaotic motions while random motions tend to equally fill the available Phase-Space [5,6,8,34].

CHAOTIC SYSTEMS, FRACTALS AND DIMENSIONS

Chaotic attractors [13,14,15,33] have the property of exponentially separating initially close trajectories in a bounded region of the Phase-Space in a time evolution of the system. A measure of this divergence is represented by the Lyapunov exponent. They quantify the sensibility to initial conditions, and for a system to be chaotic it must have at least one positive Lyapunov exponent. From this point of view the Chaotic attractor can be thought of as a noise amplifier: it brings to a macroscopic level the microscopic fluctuations. Strange attractors have another difference with respect to Attractors belonging to regular motions: they have a fractal dimension. The reader is referred to [34] for further mathematical definition of a Strange attractor. In order for the attractor to be strange, the trajectory must show sensitive dependence on initial conditions and its dimension must be a fractal greater than two.

The definition of the dimension [36] of a geometrical object is based upon the concept of measure in space and the dimension of the space in which one observes a geometric object is fundamental for the recognition of its topological properties. Whitney [38] has proven that an m-dimensional object may be embedded in a space of dimension n. The minimum space dimension for a curve (dimension 1) is 3. In fact, if a 3-dimensional curve is projected into a plane, intersections and closed areas may appear and the image does not represent a 1-dimensional object any more (**Fig. 2a**). The dimension of the space will be called the embedding dimension to distinguish it from the dimension of the object itself.

There are several definitions of dimension but only few of them are topologic in nature, in the sense that they attribute the same dimension to topologic equivalent objects.

The **Covering Dimension** is the first definition presented and it is topologic in nature. The idea is to take a geometric object and try to cover it with disks of small radius (**Fig.2b,c**). There are other definitions for the dimension of an object that are able to capture the differences in the internal structure of topological equivalent. These definitions can be divided into two groups: those which only depend on metric properties (the **Capacity dC** and the **Hausdorff Dimension dH**) and those depending on metric and probabilistic properties thus taking into account the frequency with which each region is visited by the trajectory (**Correlation Dimension**). [8,13,14,29,36].

RECONSTRUCTING PHASE-PORTRAIT FROM EXPERIMENTAL TIME SERIES. TAKENS THEOREM.

The construction of the multi-dimensional object in the Phase-Space, to characterize the state of the system is difficult. This paragraph illustrates how the time evolution of a system in the Phase-Space can be reconstructed using experimental data. Takens [35] gave full mathematical proof of the theorem whose practical implementation constitutes the so-called 'method of delays'. It states that, in order to reconstruct the Phase-Space Portrait of a system that has m degrees of freedom, one only needs to measure one of them and substitute the others with time delayed values of the measured quantity. This mapping constitutes an embedding, from the m-manifold to the Euclidean space provided that one uses at least $n = 2m+1$ delayed values. The dynamic of a single parameter contains the information about the other parameters that influence the phenomenon and therefore of all the important degrees of freedom.

If n is the embedding dimension, δ is the delay time and τ is the sampling time, then from the signal x(t) one can extract the vector x(t1), that represents a point in the in Phase-Space, whose components are n values delayed one from the other of the delay time starting from x(t1), the first data point of the time series. The following vector will correspond to the time instant $t2+\delta$ and so on to build the so-called trajectory matrix. The value N depends on the length of the time series and on the choice of the embedding parameters: if one has M data points then $N = M - n$.

However very powerful, Takens' theorem gives no hints for a practical implementation. Most of the time the experimenter is faced with a finite number of sampled data that contain noise and have a finite precision. There are no indications regarding the choice of the time scales like time delay or sampling time, any value is good in infinite algebra. The dimension of the attractor of the dynamic system is not known a priori making it difficult to satisfy the embedding requirement. Theoretically these problems are still open, especially with respect to the proper choice of the time scales and of their influences on the attractor reconstruction. Some of these problems have been discussed in [3,4] and only a few concepts will be qualitatively presented here. The necessary mathematical support can be found in the literature.

As for the choice of the sampling time, the suggestion is that of over-sampling with respect to the cut-off frequency of the anti-aliasing filter in order to smooth out trajectories, Darbyshire and Price [8]. The amount of information that is possible to extract from a sampled time series is finite. The scope of the time delay method is that of reconstructing the dynamics of the system. Therefore, all the relevant dynamics must be present in the chosen variable and the delay time should be chosen so that even the fastest modes are reconstructed.

APPLICATION TO ROTATING STALL.

The complicated phenomenon of stall, inception and stabilized unsteady conditions expresses itself by fluctuations in pressure, velocity vector, noise changes, stress variation and vibrations of the compressor. The condition of the turbomachine can be represented in a multi-dimensional space with these parameters as dimensions. The transition from one point to the next is controlled by the time step of the data acquisition. The Takens theorem, applied to a compressor, means that it is sufficient to measure one parameter and still be able to reconstruct the Phase-Space. All the information about the phenomenon is contained in each signal. An attractor can be build and the properties investigated. A few issues remain open: Does each parameter contain the full information? Otherwise one is not sure about the representative aspect of the attractor. The choice of the sensor is also dependent on these conclusions. The multi-dimensional aspect is recreated by the time delay method. How large must the time delay be? Does the resulting attractor have fractal properties? How can we preserve a maximum of information from the multi-dimensional Phase-Portrait in a simplified three-dimensional map? Which of the multi-dimensional axis should be selected for the three-dimensional representation? What about an idealized attractor, a "cleaned-up" one, which can be used as model for predictive purposes? How good can it be applied to the specific case of stall in a compressor? Do we observe pre-stall indicators by using a single sensor and does the Phase-Portrait analysis show it? If this can be demonstrated in a difficult case (rotating stall), it provides an indication of validity of the principle and maybe can be used in real time control and monitoring by using the predictive capability of the attractor.

DESCRIPTION OF EXPERIMENTS

One of the aims of this study is that of verifying the possibility of tracing the same physical phenomenon i.e. rotating stall, by measuring different physical quantities influenced by it. These are for example: flow vector fluctuations in the rotor annulus, the pressure fluctuations at the casing wall, vibrations of the casing structure, blade stresses and acoustic noise. As the technique of the Phase-Portrait construction does not require the knowledge of the absolute values of the measured quantity, no calibration of the instruments is required [4]. The data acquisition was performed on PC equipped with a Metra Byte DAS20 card. It is a multifunction high speed A/D, I/O expansion board that allows precision data acquisition and signal analysis directly on the PC. The capability of the card is of 100 kHz with 16 single or 8 differential ended input channels. The acquired data are stored in two 8 bit bytes. Between the card and the transducers an anti-aliasing low-pass filter was used.

The static pressure signal at the casing is recorded with two different sensors. The first one is a flush mounted Kulite pressure transducer. The second one is an inductive type of pressure transducer i.e. a Valydine connected to the casing pressure taps by a short tube. The displacement volume together with the dimensions of the connecting tube characterizes the unsteady response capability of this transducer. No low-pass filtering has been used in this case since the high frequencies are naturally damped. The frequency content of the signals from the microphone and the accelerometers was measured sending the non-filtered signals to a HP 35660A Dynamic Signal Analyzer. This analyzer digitally samples the B&K Signal analyzer output signal and displays, in real time, the frequency content of the analogue signal.

Preliminary experiments have been organized to determine :

1. The influence of the sensor type, hot wires, pressure transducers, vibration pick-up, microphone in the time series and the Phase-Portrait construction.
2. The determination of the fractal properties of the Phase-Portrait during stall.
3. The determination of the required delay time to apply to the time series.
4. The determination of the dimensions of the object and the embedding space.
5. The application of smoothing of the object.

6. An attempt to find the representative equations for the three axis so that an equivalent attractor is generated in a synthetic way.
7. The use of the predictive capability of a Phase-Portrait of a stall event and application to a time series.
All these aspects have been treated in the references 3,4,22,23,24,29,30,31 and 32.
The investigation of rotating stall inception is treated in this paper. The experiments have been organized to cover a transient from the clean operating point to the occurrence of rotating stall by a continuous throttling of the compressor.

ROTOR FACILITIES.

The R1 low-speed axial-flow compressor test facility at the VKI is the first presented. It is an open loop, constant annular section facility with inner conical diffuser and throttle valve. The rotor is driven by 55 KW DC motor with a continuous speed control from 0 to 1500 rpm. The tip radius is 0.704 and the hub to tip ratio is 0.78. The facility is equipped with 39 IGV, 25 rotor and 25 stator blades. Tip radius is 0.704m and hub-tip ratio 0.78. The IGV and rotor blades are of NACA 65-A10 type, while the outlet guide vanes have constant thickness, non twisted thin metal airfoils of 35 deg. camber and constant chord of 80 mm. As the mass flow is reduced, a multi-cell small stall pattern is first encountered, followed by a 1-cell and then 2-cell large stall pattern. Reopening of the throttle valve produces a 1-cell large stall pattern in the hysteresis branch of the characteristic curve [2].
Instrumentation: Hot-wire (axial and tangential position) 17mm.: upstream rotor leading edge, 7mm. from casing. Validyne and Kulite pressure transducer : 17mm. Upstream rotor LE and flush mounted.
The second facility is the R2 axial-flow compressor (**Fig. 3**). A DC motor of 180 KW power drives the rotor. The inlet is bell shaped and followed by the test chamber with the rotor and the stator. The tip diameter is 400 mm with a hub to tip ratio of 0.5. There are 24 subsonic blades of the NACA 65 family. This facility presents immediately large stall with an abrupt drop in pressure rise. The rotor starts in rotating stall for speeds from 0 to 3000 rpm . Above 3000 rpm, unstalled flow is observed at open throttle. The low compression ratio of the tested rotor and the testloop internal losses are the reason for this behavior.
Instrumentation : Hot-wire (axial and tangential position): 15mm. upstream of rotor LE; 10mm. from casing, midheight and 10mm from inner casing. Validyne and Kulite pressure transducer : 70mm. upstream of rotor LE and flush mounted.

THE STALL INCEPTION.

The stall inception can be defined as the process by which the flow trough the compressor changes from an axi-symmetric distribution to an asymmetric one; as indicated by Day [9] and by Höss et al. [18]. There are three different kinds of inceptions that can be observed for various conditions in a low pressure compressor:
1. Stall rising from a spike-type precursor,
2. Long wavy pressure fluctuations corresponding to modal waves,
3. Dominant action of the shaft unbalancing as an external forcing action.
In case of distorted inlet flow the whole velocity range is dominated by the spike-type stall inception behavior.

These very short length scale disturbances are localized only in few rotor revolutions and travel around the annulus increasing in amplitude until fully developed stall occurs.
The spike-type precursor occurs when the disturbance is small and localized to just few blade passages, in term of the circumferential length its dimensions are very small and they increase quickly until full stall conditions are established.
The long length scale disturbances, a model proposed by Emmons et al. [10] and extended to multi-stage machines by Moore and Greitzer [27], involve perturbations that are of the same scale of the circumferential length and are referred to as modal waves or "modes". According to this model of stall inception these pre-stall waves start as weak disturbances and grow in intensity without abrupt variation in amplitude or frequency until a fully developed stall cell is formed.

In order to see the stall inception, various techniques have been used. Tryfonidis et al. [37] analyzed the behavior of nine different machines (fan, core and engine compressors) using the method of the spatial Fourier analysis. They were able to identify low amplitude traveling waves prior to stall. The structure of these waves is different for different speeds and, for the same speed, depends on the position on the characteristic curve.
Höss[18], on the other side, analyzed the behavior of a two-spool turbofan engine using the wavelet analysis. The presence of the three kind of stall precursors and the importance of external influences (e. g. the shaft unbalancing) are verified.
In the present report the attention is focused on the analysis of stall inception using the Phase- Space Portraits method, without trying to identify a certain kind of stall precursor but trying to identify a possible stall warning that can be clearly seen with this technique. The different aspects will be demonstrated using one of the compressor experiments.

THE RECORDED TIME-SERIES.

Given that the purpose of this work was to carry on a qualitative analysis of the stall inception there is no need to know very accurate values for velocity and

pressure and the experimental accuracy in this case is not relevant. For that reason no calibration was done on the different sensors and the results presented here are only the digits as they were recorded by the acquisition system. This means that the data obtained with the hot-wire are not proportional to the speed values but depend on them according to King law.

a. The low speed compressor R1

The experiments are carried out at 1000 rpm. The characteristic curve (**Fig. 4a**) shows a stable part to maximum loading (point A), 7 to 10 small perturbed regions (point B). All the small stall cells grow in size and collect themselves to give origin to a single big cell (point C), the single big cell splits in two (point D). An increase of the mass flow starts the hysteresis loop and the flow becomes clean again (point A).

The axial hot-wire

The hot-wire is parallel to the axis of the machine and is sensitive to the variations of the tangential component of the velocity. After 21 rotor revolutions in the acquisition sequence, the peak-to-peak amplitude of the signal grows (**Fig. 5**). The small cells collect together into a single big cell ; this process can be seen when, after about 88 rotor revolutions, the amplitude and the relative frequency of the large peaks increase. The single big cell starts growing and is fully established at 105 revolutions. (1 horizontal.unit = 10 revs.)

The tangential hot-wire

The hot-wire is orthogonal to the axis of the machine and is sensitive to the variations of the axial component of the velocity, showing the massflow variations (**Fig. 6**). During the first 11 rotor revolutions the flow is quite clean while the mean value of the signal decreases for increasing throttling. In small stall conditions the negative peaks of the signal grow in amplitude and in relative frequency (11 to 100 rotor revolutions) while the largest oscillations are visible in deep stall conditions (from about 100 rotor revolutions on).

The Validyne pressure transducer

When the main velocity component decreases because of throttling, the wall static pressure grows as shown by the output of the transducer. The passage of a stall cell through the sensor location causes a sudden increase of the pressure (the axial speed decreases suddenly).

This can be observed in the time traces recorded with this transducer (**Fig. 7**): during the first 11 rotor revolutions the flow is clean. Between 11 and 34 rotor revolutions the throttling is causing an increase of the mean value of the pressure, but the small peaks due to the passage of the small perturbation cells are not yet evident. Between 34 and 87 rotor revolutions one picks up the small perturbations. After about 87 rotor revolutions, the small cells are collecting together and a single big cell is growing. This process takes about 20 rotor revolutions until deep stall conditions establish after 109 rotor revolutions.

The Kulite pressure transducer

A period of almost clean flow (about 10 rotor revolutions) is followed by about 30 revolutions during which there is a smooth passage from clean flow to small stall conditions. The deep stall condition starts its development around 80 revolutions and is completed at 100 revolutions in the acquisition (**Fig. 8**). A cut-off filtering is set at f_f=500 Hz.

b. The R2 compressor

The experiments are carried out at 4000 rpm. The characteristic curve is shown (**Fig. 4b**). The lack of suitable IGV's causes the rotor hub section to operate at positive and the tip one at negative incidence angle. The hub is expected to be the most critical in the stall triggering and a sudden occurrence of deep stall is observed. Experiments at three radial positions (hub, mean and tip) are carried out.

The axial hot-wire

From the results obtained it can be deduced that the behavior of R2 is quite different from the one seen with the R1 compressor. No small perturbations of increasing amplitude up to stall are observed and deep stall occurs quite suddenly. The axial hot-wire is sensitive to the variations of the tangential component of the velocity. No perturbations are detected until stall conditions are established at the three radial positions.

The tangential hot-wire

The sensor is sensitive to the axial component of the velocity and shows the reduction of the mass flow for increasing throttling. The mean value of the output of the wire decreases until stall conditions cause the wide fluctuations of the signal for hub and tip radius(**Fig. 9a,b**). (1 horizontal.unit = 40 revs.for all R2 figs.)

The Validyne pressure transducer

The wall pressure increases (**Fig. 10**); again there is no sudden variation in flow condition up to full stall, where the passages of the stall cells are clearly visible.

The Kulite pressure transducer

The higher frequency response of this provides the time trace of **Fig. 11**. The evolution of the stall transient is quite similar to the one recorded with the Validyne.

THE PHASE-SPACE PORTRAITS.

The in-house developed routines for the evaluation of the average mutual information (as function of the time delay) and of the false nearest neighbors' percentage (as a function of the dimensions) respectively are used. The value of τ_d (time delay) and ED (embedding dimension) are used for the application of the Takens principle and the construction of the Phase-Space. In this kind of analysis a steady state condition is represented by a single point in the Phase-Space, while small oscillation of the data around a constant mean value will be represented by a cluster of points contained in a relatively small region. If the mean value changes the center of this cluster moves. Finally big oscillations are

represented by a set of points contained in a larger region. These Phase-Space portraits are derived from the time series discussed in the previous paragraph.

a. The low speed compressor R1

The axial hot-wire

The analysis of these data gave the following parameters: $\tau_d = 50\tau_s$ and ED = 5

(τ_d : time delay , τ_s : sampling time , ED = embedding dimension.)

The 3-D reconstructed portrait is shown in **Fig. 12**. Given that the mean value of the time trace doesn't change too much during the first part of the transient, what can be expected is a gradual growth in size of the region that contains the portrait.

In a 2-D projection there is an increase of the size of the region that represents the operation before deep stall. The small perturbations cause an increase of the peak-to-peak amplitude of the sensor output without changing too much the mean value.

From this analysis, it can be inferred that a possible application for a monitoring system consists in looking at a bounded sub-domain of the Phase-Space that contains the portrait of the system in clean flow. In this way the stall warning should be activated when the portrait goes out of this control volume.

The tangential hot-wire

The reconstruction of the Phase-Portrait is done using: $\tau_d = 44\tau_s$ and ED = 5

A 3-D projection of the portrait is shown in **Fig. 13**; the situation here is quite different from the previous one because now the main variation can be seen in the mean value of the time trace.

From the analysis of this Phase-Portrait it could be inferred that a possible monitoring system that uses this sensor could check the motion of the center of the portrait and give a stall warning when it goes over a certain distance from its original position.

The Validyne pressure transducer

The reconstruction of the Phase-Portrait used: $\tau_d = 49\tau_s$ and ED = 5. The 3-D projection of the portrait is shown if **Fig. 14** and there is a wide displacement of the geometrical center during the transition to stall and compared with the operating conditions A,B,C, and D.

During the first 20 rotor revolutions the mean value of the signal doesn't change much and the displacement of the center of the portrait is relatively small as well as the size graph (clean flow means small peak-to-peak amplitude of the signal). During the period between 20 and 35 rotor revolutions there is a displacement of the center due to the decrease of the mass flow, proportional to the mean value of the signal. The next step (from 35 to 88 rotor revolutions) shows a large displacement of the graph center while there is an increase of its size because of the increased fluctuations of the time trace (small perturbations). Finally, the large size of the portrait is caused by the large fluctuations of the time trace during deep stall.

As it can be seen comparing the portraits, the large displacement of the graph center is such that the common areas between the preceding step and the following one are very small.

The Kulite pressure transducer

The reconstruction is carried out using: $\tau_d = 49\tau_s$ and ED = 5. The 3-D projection of the Phase-Portrait is shown in **Fig. 15**; this object is very similar to the one obtained in the case of the Validyne. These transducers are measuring the same variable, wall static pressure, and the main characteristic of the reconstructed portrait should be the same as well as the required time delay. The similarity of the portraits indicates that all information about the chaotic evolution is contained in low frequency. The faster response of the Kulite provides more details on the unsteady motion.

A second small cluster appears in deep stall condition, at a position close to the portrait obtained in clean flow. The "steady" reverse flow in the core of the stall cell is treated in this representation as a "clean" condition. It is also an illustration for the need of the correct embedding. The two "stable" conditions are not clearly separated in a 2-D projection, while the 3-D view reveals that they are different structures.

b. The R2 compressor

The axial hot-wire

The experiments are carried out at three different radial positions and three phase portraits can be built, after the calculation of the average mutual information and the false nearest neighbors. The time delay is between 45 and 49, while the embedding dimension is 5. The clean flow condition is represented by a cluster of points, around a mean value. When stalled flow conditions occur, the portrait suddenly explodes (**Fig. 16**). The main difference between the hub and tip portraits is in the size of the initial cluster because of the higher fluctuations of the time trace recorded near the tip.

The tangential hot-wire

From the analysis of the 3D projections of the portraits taken near the hub and near the tip (**Figs. 17**) it is clear that the main characteristic of the motion is the variation of the mass flow. The displacement of the center is very large, the size of the graph doesn't increase too much for increasing peak-to-peak amplitude of the time trace.

The Validyne and Kulite pressure transducer

The behaviour of both pressure transducers is similar and is similar to what already shown with the tangential hot-wire. , In both cases the main phenomenon that can be seen in the time series is the variation of the mean value of the signal, while the peak-to-peak amplitude changes only when stall occurs. The 3D projections of the portraits are shown in **Figs. 18, 19**. Like in the case of the R1 compressor, the similarities between the two portraits are a indication that interesting information on chaotic motion is also present in the low frequency.

CONCLUSIONS.

A clear advantage of this method is the fact that there is no need for a calibrated instrument, what has been analyzed is the raw output of sensor.

The embedding dimension has been evaluated between 5 and 6 for all the sensors and for the compressors investigated. The percentage of false nearest neighbors is very low in the fifth dimension, probably this "degree of freedom" is more affected by measurement noise then by the physical information.

The data acquisition has to be performed in real time and the reconstruction of the portrait done, giving in advance the values of the time delay and of the embedding dimension.

The speed by which the point moves on the stable part of the portrait is an indication for the proximity to stall during a transient.

From the analysis of the signals recorded on the R2 facility what comes out is that a monitoring system based on the displacement of the center of the portrait should have better performances then the one based on the check of the size because the sudden instability leaves almost no time for a control.

This concept has to be verified on transonic fan type and multistage compressors.

BIBLIOGRAPHY.

1. **Abarbanel, H., et al.**; "The analysis of observed chaotic data in physical systems." Reviews of Modern Physics, 65(4), October 1993.

2. **Breuer, T.**; "Compressor Flow Instabilities Part II: Analysis Techniques", VKI-LS 1996-05 "Unsteady Flows in Turbomachines" , Brussels, March 11-15 1996.

3. **Breugelmans, F.A.E., Palomba, C.**; 1998, "Recherche récente en décrochage tournant : Chaos, Fractales et Attracteurs." Revue Française de Mécanique, N° 1998-4. 31 Décembre 1998.

4. **Breugelmans, F.A.E., Palomba, C. and Funk, T.**; 1994, "Application of strange attractors to the problem of rotating stall rotating stall", 7th ISUAAT, September 25-29, Fukuoka, Japan (Elsevier)

5. **Broomhead, D.S., and King, G.P.**; 1992, "Extracting qualitative dynamics from experimental data", Physica 20D, pages 217-236.

6. **Broomhead,D.S., and King, G.P.**; "Singular system analysis with application to dynamical systems" Physica D, 20:217, 1986.

7. **Cawley, R., and G. H. Hsu, G.H.**; "Local-geometric-projection method for noise reduction in chaotic maps and flows". Physical review A, 46(6):3057, September 1992.

8. **Darbyshire, A.G., Price, T.J.**; 1991, "Phase-Portraits from chaotic time series", Fractals and Chaos, ed. Crilly, Springer, pages 247-257.

9. **Day, I.J.**; "The fundamentals of stall and surge in axial compressors." VKI-LS 1996-05 "Unsteady Flows in Turbomachines" , Brussels, March 11-15 1996.

10. **Emmons, H.W., Pearson, C.F., Grant.H.P.**; "Compressor surge and stall propagation." Transactions of the ASME, vol.77, pages 455-469, 1955.

11. **Garnier, V. H ., Epstein, A. H., Greitzer, E. M.**; "Rotating Waves as a Stall Inception Indication in Axial Compressors", Journal of Turbomachinery, vol. 113, April 1991, pages 290-302.

12. **Garnier, V., Escuret, J.F., Previtali, R. e Duvaut, P.**; "Stall Inception Measurements in the High-Speed Multi-Stage H4 Compressor." VKI LS "Unsteady Flows in Turbomachines" 1996-05, Brussels, March 11-15 1996.

13. **Grassberger, P., Procaccia, L.**; "Measuring the Strangeness of Strange Attractors" , Physica 9D, 1983, pages 189-208.

14. **Grebogi, C., Ott, E., Yorke, J.A.**; 1987, "Chaos, strange attractors and fractal basin boundaries in nonlinear dynamics", Science, vol. 238, October, pages 632-638.

15. **Grebogi, C., Ott, E., Pelikan, S., Yorke, J.A.**; 1984, Physica 13D, page 261.

16. **Greitzer, E.M. and Moore, F.K.**, 1986, "A theory of post stall transients in axial compression systems: Part 11-Application", ASME Journal of Engineering for Gas Turbines and Power, vol. 108, pages 231-239.

17. **Gu, C., Yamaguchi, K., Nagashima, T., Higashimori, H.**; 1999, "Observation of Centrifugal Compressor Stall and surge in Phase-Portraits of Pressure Time Traces at Impeller and Diffuser Wall." The International Gas Turbine Congress 1999 Kobe, pages 555-560.

18. **Höss, B., Leinhos, D., Fottner, L.**; "Stall inception in the compressor system of a turbofan engine." Proceedings of the Gas Turbine & Aeroengine Congress & Exhibition, Stockholm, June 1998.

19. **Inoue, M., Kuroumaru, M., Iwamoto, T., Ando, Y.**; 1991, "Detection of Rotating Stall Precursor in Isolated Axial Flow Compressor Rotors", ASME Journal of Turbomachinery, vol. 111, pages 281-289.

20. **Jakson, A. D.**; 1987, "Stall Cell Development in Axial Compressor", ASME Journal of Turbomachinery, vol. 109, No 4 pages 492-498.

21. **Mandelbrot, B.**;"The fractal geometry of nature", W.H. Freeman and company, page 15.

22. **Mathioudakis, C.**; "Rotating stall in axial flow compressors", PhD Thesis K.U.Leuven, 1985

23. **Mathioudakis, K., Breugelmans, F.A.E.**; 1985, "Development of Small Rotating Stall in a Single Stage Axial Compressor", ASME paper, 85-GT-227.

24. **Mathioudakis, K., Breugelmans, F.A.E.**; "Three dimensional flow in deep rotating stall cells of an axial compressor." Journal of Propulsion and Power, vol. 4,n0 3, pages 263-269, June 1988.

25. McCaughan, F.E.; 1994, "When are nonlinearities important at stall inception?", ASME 94-GT-338.
26. McCaughan, F.E.; 1989, "Application of bifurcation theory to axial flow compressor instability", Transaction of the ASME, vol. I I 1, October, pages 426-433.
27. Moore, F. K., and Greitzer, E. M.; 1986, "A Theory of Post-Stall transients in Axial compressors: Part I - Developments of the Equations", ASME Journal of Engineering and Power, vol. 108, pages 68-76.
28. N. H. Packard, N.H., et al.; "Geometry from a time series." Physics Review Letters, 45:712, 1980.
29. Palomba, C.; "L'Analisi sperimentale dello stallo rotante secondo le techniche della teoria del caos deterministo." PhD Thesis, Universita Degli Studi Di Cagliari, July 1997.
30. Palomba, C., Breugelmans F.A.E.; "Phase-Portraits from Rotating Stall Time Series."
XII ISABE Conference, Melbourne Australia Sept. 1995.
31. Palomba, C., Puddu, P., Breugelmans, F.A.E., Nurzia, F.;. "Caratterizzazione delle Condizioni di Funzionamento di un Compressore Assiale in Prossimita' dello stallo rotante secondo le tecniche della Teoria del Caos." Proceedings of the Conference Turbomachine 96' Genova 11-12 July 1996, pages 761-772.
32. Palomba, C., van der Horst, L., Breugelmans, F.A.E.; " Strange Attractor Characte-risation of Rotating Stall in an axial flow Compressor." JSME Centennial, July 1997 Tokyo.
33. Peitgen, H.O., Jiirgens, H., Saupe, D.; 1992 "Chaos and Fractals, new frontiers of science", Springer Verlag New-York, Inc. pages 106-119.
34. Schuster, H.G.; 1984, "Deterministic Chaos", Physic Verlag – Weinheim.
35. Takens, F.; 1981, " Detecting strange attractors in turbulence", Lecture Notes in Mathematics, Rand and Young eds. Springer, Berlin 1981, page 366.
36. Theiler J.; "Estimating Fractal Dimension." Journal Optical Society, vol.7, No. 6, June 1990, pages 1055-1073.
37. Tryfonidis, M., Etchevers, O., Paduano, J.D., Epstein A.H., Hendricks, G.J.; "Prestall Behaviour of Several High Speed Compressors", Journal of Turbomachinery, vol. 117, January 1995, pages 62-80.
38. Whitney, H.; 1936, "Differentiable Manifolds", Ann. Math. 37, page 645.

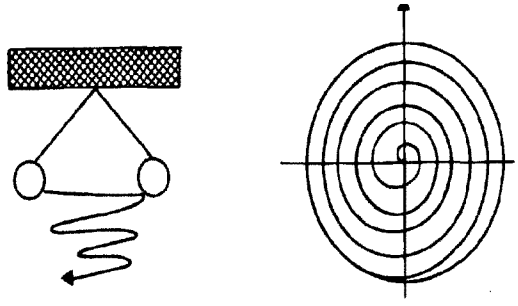

Fig. 1 Pendulum and Phase-Space Portrait

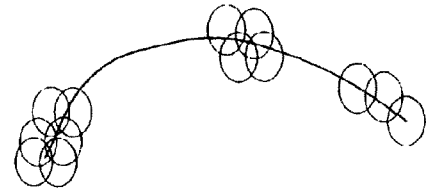

Fig. 2b. Covering Dimension – Line

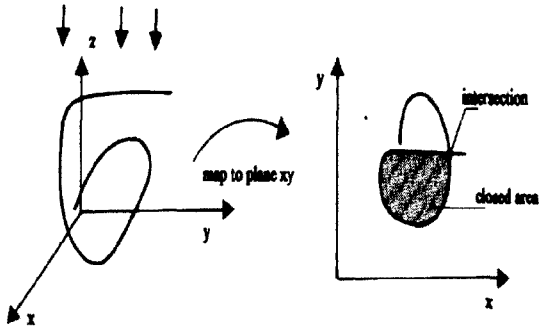

Fig. 2a. Presentation Dimension

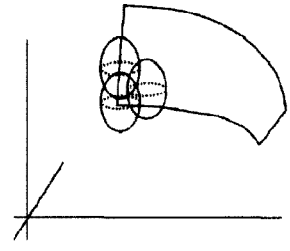

Fig. 2c. Covering Dimension – Surface

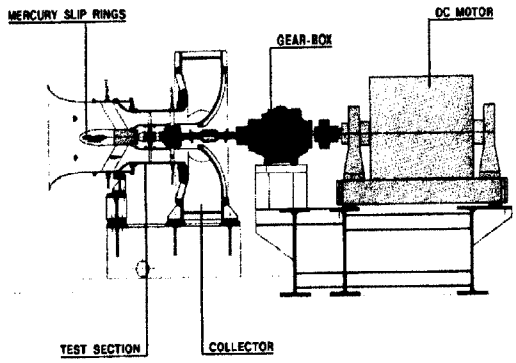

Fig. 3. R2 Compressor test facility

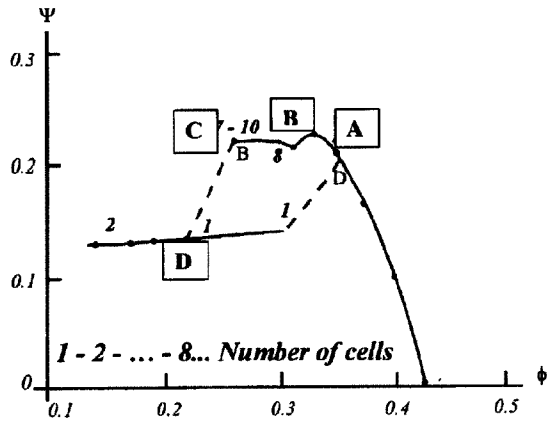

Fig. 4a. R1 Characteristic curve

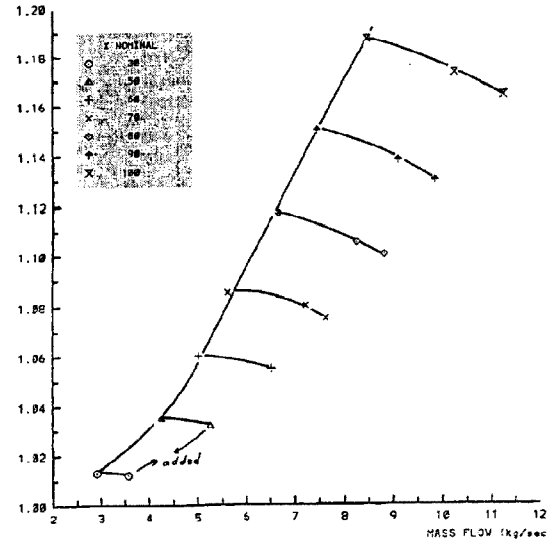

Fig. 4b. R2 Performance map.

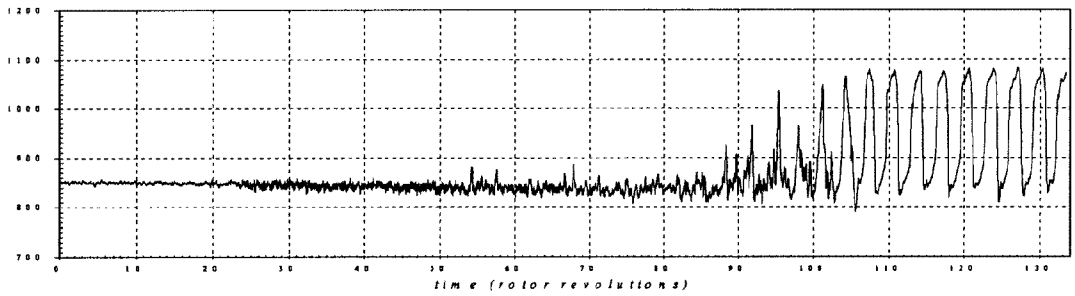

Fig. 5. R1-Time trace – Hot-wire axial position

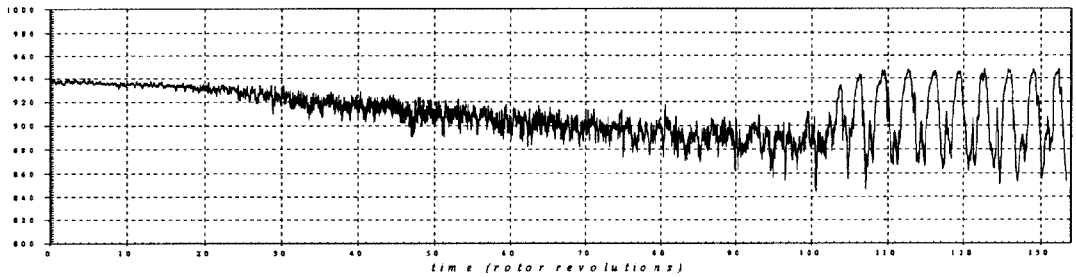

Fig. 6. R1-Time trace – Hot-wire tangential position

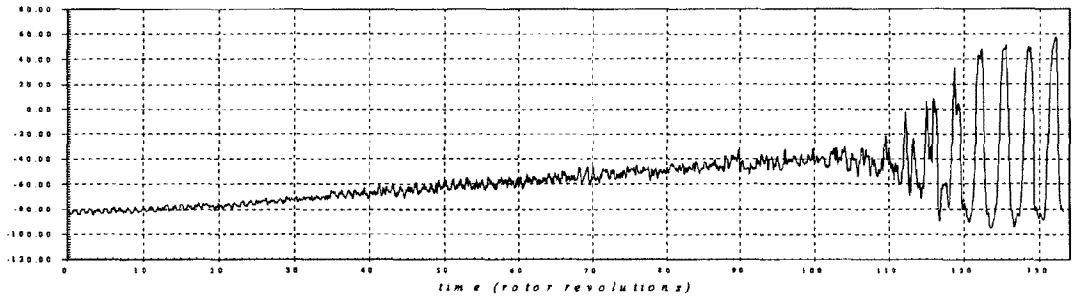

Fig. 7. R1-Time trace – Validyne pressure transducer

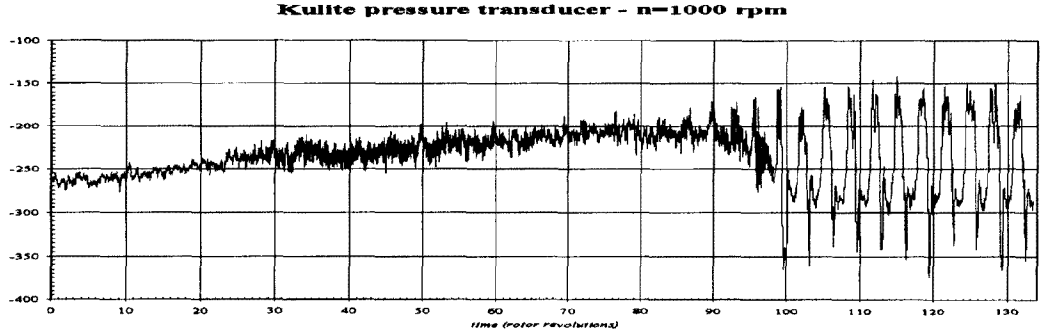

Fig. 8. R1-Time trace – Kulite pressure transducer

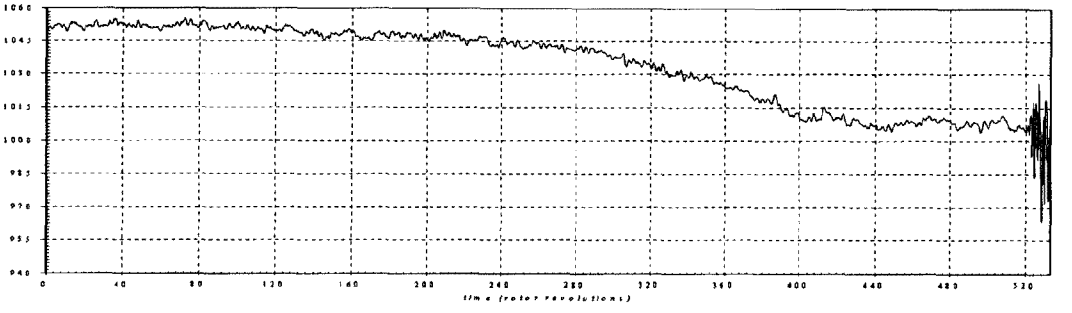

Fig. 9a. R2-Time trace – Hot-wire tangential position-Hub

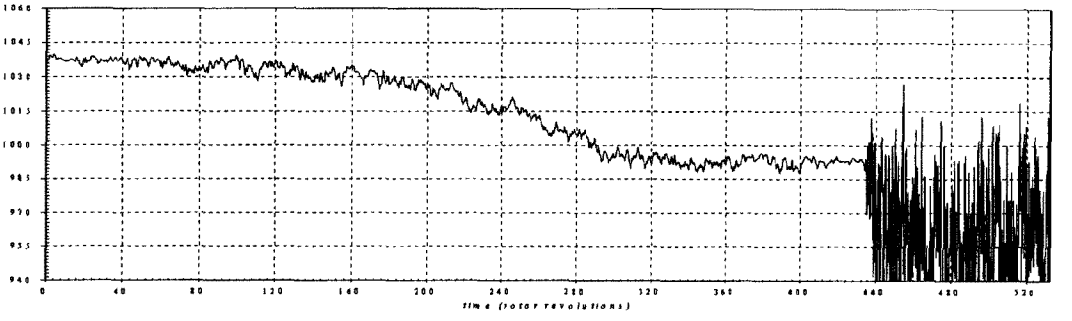

Fig. 9b. R2-Time trace – Hot-wire tangential position-Tip

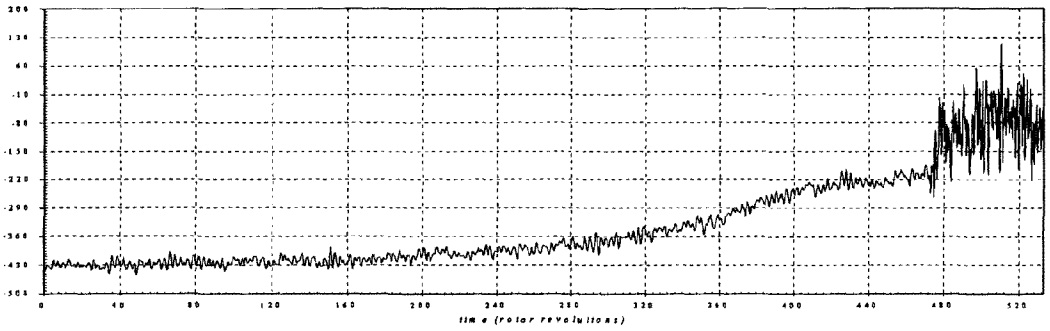

Fig. 10. R2-Time trace – Validyne pressure transducer

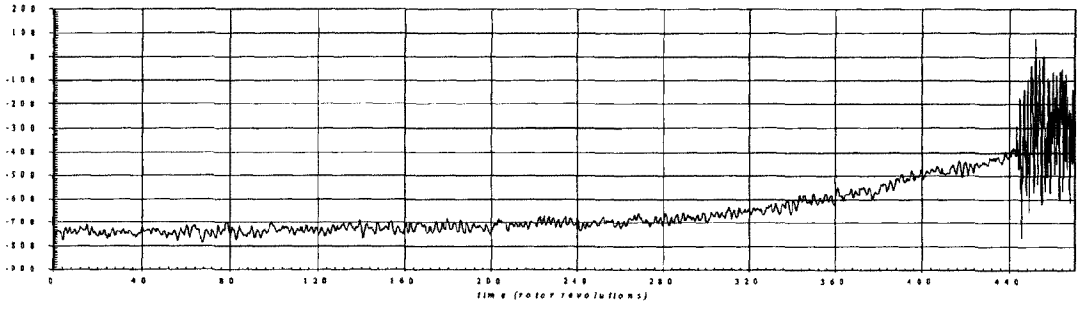

Fig. 11. R2-Time trace – Kulite pressure transducer

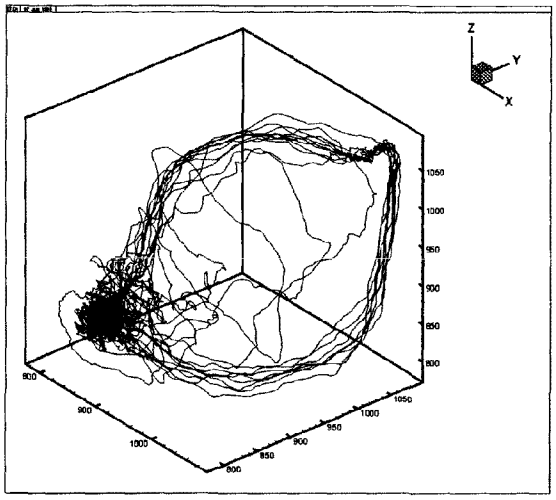

Fig. 12. R1-3-D Projection of Phase-Space portrait - Hot-wire axial position.

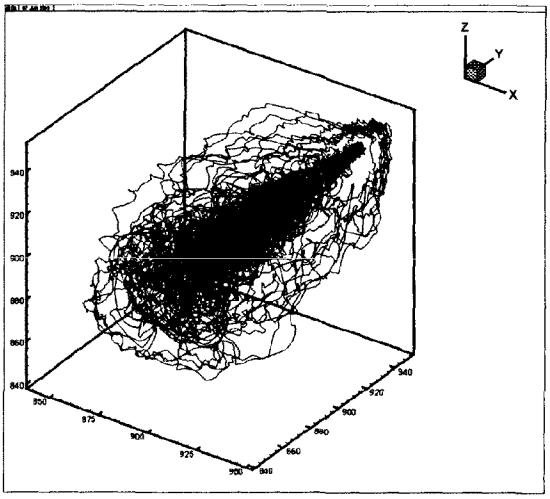

Fig. 13. R1-3-D Projection of Phase-Space portrait - hot-wire tangential position.

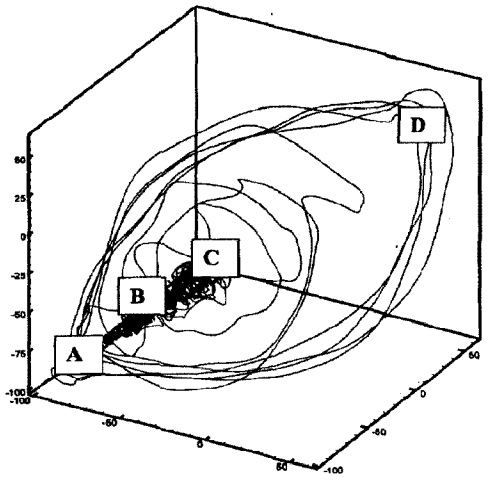

Fig. 14. R1-3-D Projection of Phase-Space portrait -Validyne pressure transducer.

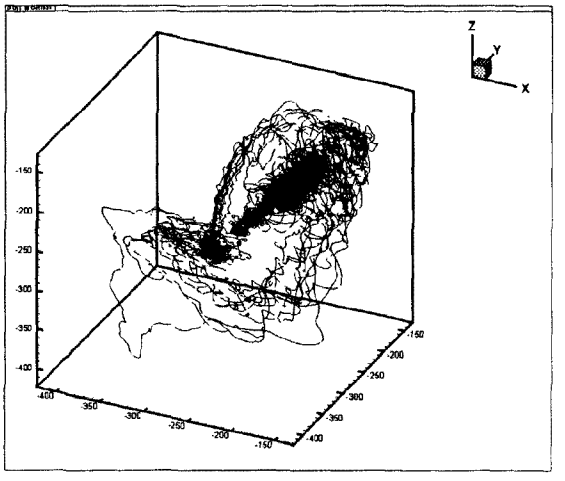

Fig. 15. R1-3-D Projection of Phase-Space portrait from Kulite pressure transducer.

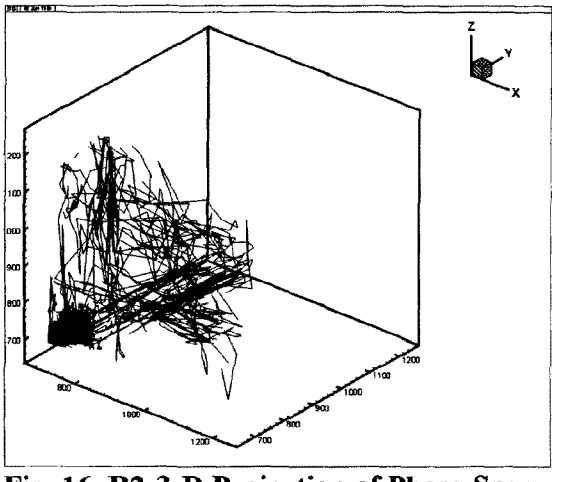

Fig. 16. R2-3-D Projection of Phase-Space portrait - Hot-wire axial position.

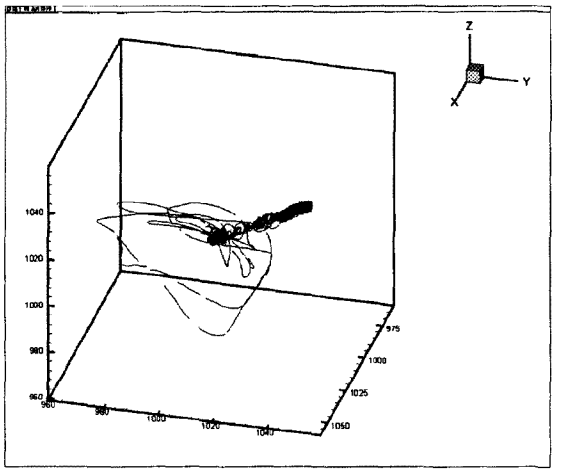

Fig. 17. R2-3-D Projection of Phase-Space portrait-hot-wire tangential position - hub.

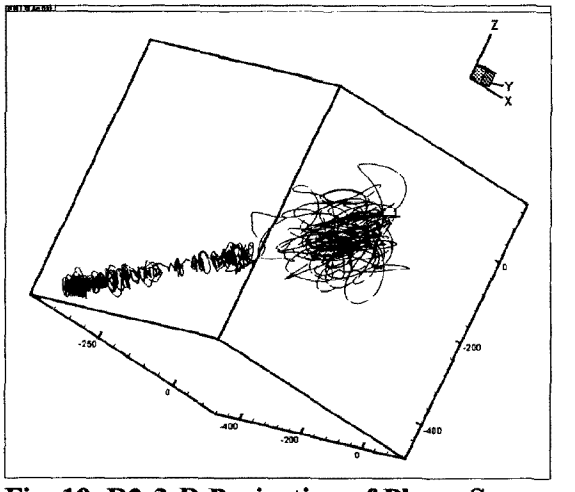

Fig. 18. R2-3-D Projection of Phase-Space portrait -Validyne pressure transducer.

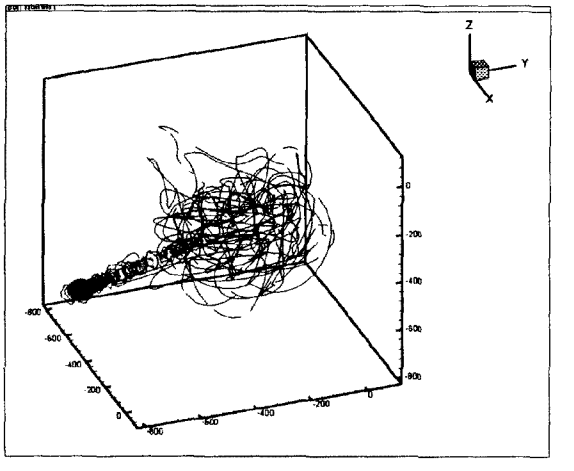

Fig. 19. R2-3-D Projection of Phase-Space portrait from Kulite pressure transducer.